JOURNAL OF QUATERNARY SCIENCE (2003) **18**(7) 663–679

Published online in Wiley InterScience (www.interscience.wiley.com). DOI: 10.1002/jqs.788

Lake stratigraphy implies an 80 000 yr delayed melting of buried dead ice in northern Russia

MONA HENRIKSEN,[1]* JAN MANGERUD,[1] ALEXEI MATIOUCHKOV,[2] AAGE PAUS[3] and JOHN INGE SVENDSEN[1]
[1] Department of Earth Science and The Bjerknes Centre for Climate Research, University of Bergen, Allégaten 41, N-5007 Bergen, Norway
[2] VSEGEI (National Geological Institute), Sredny pr. 74, St. Petersburg 199026, Russian Federation
[3] Department of Botany and The Bjerknes Centre for Climate Research, University of Bergen, Allégaten 41, N-5007 Bergen, Norway

Henriksen, M., Mangerud, J., Matiouchkov, A., Paus, A. and Svendsen, J. I. 2003. Lake stratigraphy implies an 80 000 yr delayed melting of buried dead ice in northern Russia. *J. Quaternary Sci.*, **Vol. 18** pp. 663–679. ISSN 0267-8179.

Received 4 February 2003; Revised 7 July 2003; Accepted 10 July 2003

ABSTRACT: Sediment cores from lakes Kormovoye and Oshkoty in the glaciated region of the Pechora Lowland, northern Russia, reveal sediment gravity flow deposits overlain by lacustrine mud and gyttja. The sediments were deposited mainly during melting of buried glacier ice beneath the lakes. In Lake Kormovoye, differential melting of dead ice caused the lake bottom to subside at different places at different times, resulting in sedimentation and erosion occurring only some few metres apart and at shifting locations, as further melting caused inversion of the lake bottom. Basal radiocarbon dates from the two lakes, ranging between 13 and 9 ka, match with basal dates from other lakes in the Pechora Lowland as well as melting of ice-wedges. This indicates that buried glacier ice has survived for ca. 80 000 years from the last glaciation of this area at 90 ka until about 13 ka when a warmer climate caused melting of permafrost and buried glacier ice, forming numerous lakes and a fresh-looking glacial landscape. Copyright © 2003 John Wiley & Sons, Ltd.

KEYWORDS: dead ice; lake sediments; deglaciation; Weichselian; northern Russia

Introduction

The northern part of the Pechora Lowland, northeastern European Russia (Fig. 1), is characterised by a fresh glacial landscape with numerous, irregular lakes of different sizes (Astakhov *et al.*, 1999). The hummocky landscape includes many distinct, ice-pushed morainic ridges and other glacial features. In this respect the landscape resembles the lowlands of northern Europe and North America that were glaciated during the Last Glacial Maximum (LGM) about 20 ka.

The glacial chronology of this part of northern Russia is based on radiocarbon dates and extensive use of OSL dates, and it is now demonstrated that the last glaciation occurred 60–50 ka in the western part of the Pechora Lowland and 90–80 ka further to the east (Henriksen *et al.*, 2001; Mangerud *et al.*, 2001, in press). During the LGM the southern limit of the Barents-Kara ice sheet was located off the present coastline in the Barents Sea (Svendsen *et al.*, 1999, submitted; Polyak *et al.*, 2000; Gataullin *et al.*, 2001).

* Correspondence to: M. Henriksen, Department of Earth Science, University of Bergen, Allégaten 41, N-5007 Bergen, Norway.
E-mail: mona.henriksen@geo.uib.no

Contract/grant sponsor: Research Council of Norway.
Contract/grant sponsor: European Community Environment and Climate Research Program; Contract/grant number: ENV4-CT97-0563.
Contract/grant sponsor: European Science Foundation's QUEEN.

Our strategy was to core sediments in glacial lakes in order to (i) obtain minimum ages of the deglaciation and (ii) to study the palaeoenvironmental development during the subsequent ice-free glacial period. Thus we expected to reach at least back to the Middle Weichselian (Valdai) in lakes formed by melting of buried glacier ice, where the interpretation of lake genesis was based on the geomorphological setting. After several attempts it emerged that the lowest part of the cored lacustrine sequences were much younger, thus not dating the deglaciation of the region but the climatic warming causing melting of ground ice tens of thousands years after the deglaciation. The results presented in this paper suggest that the present landscape started to form about 13 ka when extensive fields of buried ice surviving in the permafrost during the entire Middle and Late Weichselian started to melt. It is noteworthy that we managed to obtain a core reaching beyond the Eemian (Mikulino) from a lake that is situated outside the Early Weichselian ice limit. This latter core will be described in another paper.

Today permafrost is found in the northern part of the Pechora Lowland and along the Urals (Fig. 1) (Brown *et al.*, 1997). In the Late Weichselian the permafrost area extended around 20° of latitude southward, whereas during the Holocene climatic optimum the zone of discontinuous permafrost was preserved only along the coast east of Pechora River and the zone of continuous permafrost was restricted to the Yugorski Peninsula and eastward (Baulin *et al.*, 1984). During the late Holocene the permafrost expanded southward again to its present distribution.

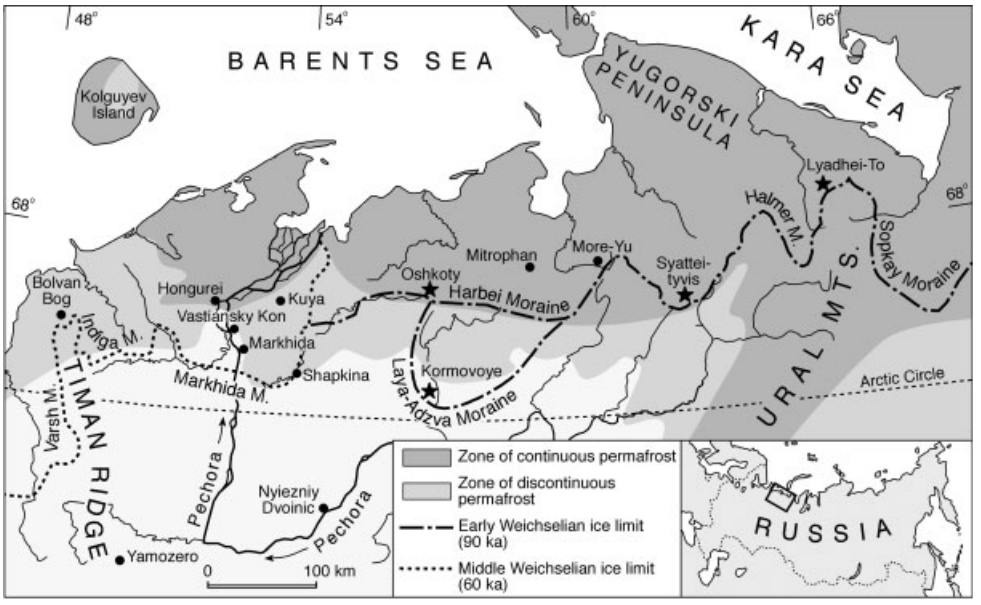

Figure 1 Map of the Pechora Lowland in northern European Russia, located between the Ural Mountains and the Timan Ridge. Sites described in this paper are marked with a star, other sites mentioned are also marked. The present interpretation of the Barents–Kara ice-sheet limits in the Early Weichselian (Harbei, Halmer and Sopkay Moraines, ca. 90 ka) and the Middle Weichselian (Markhida, Indiga and Varsh Moraines, ca. 60 ka) are shown, as well as the zones of continuous and discontinuous permafrost (after Brown *et al.*, 1997). Box on the inset map shows the location

Methods

Coring was carried out from lake-ice during the winters of 1998 and 1999. The uppermost 1–2 m of soft sediments were sampled with a hand-driven Russian peat corer. For the deeper parts we used heavy motorised geotechnical drilling equipment (UGB-50) yielding core segments 1 m long with a diameter of 10 cm. Personnel from the Usinsk Division of the Polar Ural Geological Expedition carried out the coring operations under our guidance. Cores 1–12 were recovered from Lake Kormovoye in 1998 and cores 13–21 from Lake Oshkoty in 1999. Sediments were collected in PVC tubes, mounted inside the steel core tube. Because the PVC tubes rotated during drilling some artificial shear planes were created in the sediments. Coring occasionally also caused other deformation of the sediments owing to friction and pressure, usually yielding structures confined to the mid-axis of the cores. Sediment that intruded the coring device on its way down to the sample depth was squeezed out through a hole in the upper end of the PVC tubes. However, if some of the intruded sediments remained in the coring device, there would not be enough space to sample the desired 1 m of sediment. Special attention was given to the identification of such dislocated sediments in the upper part of each core metre. Some of the cores were split and described in the field (cores 6, 7, 19 and 20). All cores were transported in a thawed condition to St Petersburg and on to Bergen, Norway, for analysis. The water depths in the lakes were measured with ropes lowered through holes drilled in the ice.

Whole core magnetic susceptibility (MS) was measured with a Bartington MS2 instrument using a 125-mm diameter sensor loop. In contrast to Lake Oshkoty, no clear correlation of the MS values between the cores in Lake Kormovoye was found and the results for this lake are therefore not presented.

The cores were split, photographed and described. Shear strength was determined immediately by fall-cone test. The results were mainly used to identify dislocated sediments, which are normally softer, and these are recorded as gaps in the logs. Sediment samples were taken at about 10-cm intervals for water-content measurements and grain-size analyses. Grain-size analyses were conducted using wet sieving of the >0.063 mm fraction, and the <0.063 mm fraction was measured by a SediGraph 5100. A Munsell soil colour chart was used for sediment colour description. Weight loss on ignition (LOI) was measured by drying samples overnight at 105°C and igniting them at 550°C for 1 h.

Pollen was analysed from core 9 from Lake Kormovoye with some additional samples from core 7 for correlation purposes. Core 9 is divided into five local pollen assemblage zones; two hiatuses and dislocated sediments were also identified from the pollen stratigraphy. The pollen samples were prepared by standard methods (Fægri and Iversen, 1989), and the computer program CORE 2.0 (P.E. Kaland and Ø. Natvik, 1993, unpublished) produced the pollen diagrams.

To obtain high precision AMS radiocarbon dating (Table 1), we hand-picked plant remains with a dry weight of >10 mg. For most samples we included only identified terrestrial plant remains to avoid any hard water effect. But for a few samples we were not able to find enough terrestrial macrofossils, and had to include some aquatic macrofossils (Table 1). The radiocarbon dates have been calibrated using the program CALIB (version 4.1) of Stuiver and Reimer (1993); however, in the text only radiocarbon ages are used.

Fluvial and glaciofluvial sand were dated by optically stimulated luminescence (OSL) carried out at the Nordic Laboratory for Luminescence Dating (Aarhus University) at Risø National Laboratory, Denmark, by A. S. Murray (Table 2). Equivalent doses were measured using the single aliquot regenerative (SAR) dose protocol applied to 200 μm quartz grains (Murray and Wintle, 2000). The dose rates were determined using laboratory gamma spectrometry (Murray *et al.*, 1987; Olley *et al.*, 1996). Water content corrections (assuming saturation because of permafrost) and calculated cosmic ray contributions are included in the dose rate data.

Table 1 Radiocarbon dates. The laboratories are: ETH—Zürich, Switzerland; LU—St Petersburg University, Russian Federation; Beta—Beta Analytic Inc., USA; T—Trondheim; TUa—prepared at Trondheim, Norway, and measured at the accelerator in Uppsala University, Sweden

Laboratory number	Sample number PECHORA	Core	Depth (cm)	Site (unit)	Material dated	^{14}C age ± 1 SD (years BP)	δ^{13}C (‰ PDB)	Maximum and minimum of calibrated age ranges, 1 SD (yr BP)[a]
ETH-22057	07-02/12	7	162	Lake Kormovoye (B6)	Twig	3990 ± 65	−28.4	4527–4410
ETH-23899	07-03/32	7	282	Lake Kormovoye (B3)	Slightly weathered twigs with bark, fruits	11 430 ± 85	−31.7	13 767–13 178
ETH-23900	08-02/22	8	272	Lake Kormovoye (B4)	Twigs with bark (four burnt), bark particles	10 175 ± 75	−26.9	12 110–11 604
T-13818	08-03/101	8	451	Lake Kormovoye (B4)	Twig	9800 ± 75	−28.5	11 231–11 170
Beta-12374	08-04/51	8	501	Lake Kormovoye (B4)	Bulk (sieved at 125 mm)	9850 ± 50	−28.0	11 254–11 197
ETH-20833	09-01/60	9	110	Lake Kormovoye (C1)	Twigs with bark, *Betula* catkin, *Picea* needles, wood particles	4185 ± 60	−28.1	4832–4586
ETH-20834	09-01/70	9	120	Lake Kormovoye (C1)	*Picea* and *Salix* wood particles	4065 ± 60	−27.6	4787–4442
ETH-20835	09-01/75	9	125	Lake Kormovoye (C1)	*Picea* needles	4310 ± 60	−30.2	4956–4833
ETH-22058	09-02/35	9	185	Lake Kormovoye (B6)	Twigs, moss stems (aquatic?)	4170 ± 75	−22.7	4832–4550
ETH-20836	09-02/70	9	220	Lake Kormovoye (B5)	Fruits of *Betula, Carex* and grass, twigs, particles of wood and bark	9420 ± 75	−29.7	10 738–10 558
ETH-20837	09-03/13	9	230	Lake Kormovoye (B5)	Bark of *Betula* or *Salix*, fresh looking wood particles	9010 ± 70	−24.6	10 223–10 154
ETH-20838	09-03/20	9	240	Lake Kormovoye (B5)	Fruits of grass, particles of wood	9615 ± 75	−25.9	11 164–10753
ETH-20839	09-03/95	9	345	Lake Kormovoye (B3)	Fresh looking particles of wood and bark, fragments of leaves	10 980 ± 80	−27.2	13 134–12 892
ETH-20840	09-04/35	9	385	Lake Kormovoye (B3)	Fresh looking particles of wood and bark, fragments of leaves	11 610 ± 85	−22.2	13 813–13 446
ETH-20841	09-04/40	9	390	Lake Kormovoye (B3)	Weathered twig	11 730 ± 85	−26.2	13 844–13 496
ETH-20842	09-06/5	9	555	Lake Kormovoye (B2)	Weathered twig	11 645 ± 85	−25.0	13 821–13 458
ETH-20843	19-12/85	19	1100	Lake Oshkoty (E)	Leaves (*Dryas octopetale*), moss stems, fruits, fresh looking particles of wood and bark	12 320 ± 90	−29.0	15 307–14 131
ETH-25566	21-15/80	21	1450	Lake Oshkoty (E)	Leaves (*Dryas octopetale*), moss stems, fruits, fresh looking particles of wood and bark	11 370 ± 80	−26.1	13 458–13 162
LU-4285	99-3255			Yanemdeityvis	Bulk of organic detritus	10 610 ± 180		12 909–12 304
LU-4284	99-3256			Yanemdeityvis	Wood	9360 ± 70		10 685–10 430
LU-4283	99-3265			Yanemdeityvis	Bulk of peat	6620 ± 60		7569–7431
TUa-1515	96-2043			Nyiezniy Dvoinic	Peat within ice wedge cast	10 335 ± 225	−29.3	12 805–11 575
T-13051	96-0008			Shapkina, section 10	Peat within ice wedge cast	11 315 ± 140	−28.9	13 453–13 143
T-13053	96-0011			Shapkina, section 10	Peat within ice wedge cast	10 195 ± 105	−27.7	12 296–11 579
T-11199A	93-15/3			Shapkina, section 11	Organic matter within ice wedge cast	9515 ± 270	−25.2	11 195–10 420

[a] Calibration data set from Stuiver *et al.* (1998).

Table 2 Optically simulated luminescence (OSL) dates on quartz, using the sand grain fraction. All the dates are from the Nordic Laboratory for Luminescence Dating, Risø, Denmark

Risø laboratory number	Field number PECHORA	Site	Sediment, stratigraphy, etc.	Age ± 1 SD (ka)	Equivalent dose (Gy)	*n*	Annual dose rate (Gy kyr^{-1})	Water content (%)
002507	98-0041	Lyadhei-To	Laminated silty fine sand, kame sediments; depth 1.2 m	87 ± 5	173 ± 1	15	2.00 ± 0.11	27
022526	98-0040	Lyadhei-To	Ripple laminated fine to medium sand, kame sediments; depth 3.5 m	114 ± 8	183 ± 9	27	1.61 ± 0.07	28
022525	98-0039	Lyadhei-To	Ripple laminated fine to medium sand, kame sediments; depth 4.7 m	125 ± 8	230 ± 10	27	1.85 ± 0.07	30
002506	98-0038	Lyadhei-To	Ripple laminated fine sand, kame sediments; depth 8.0 m	120 ± 8	198 ± 3	15	1.65 ± 0.09	27
002528	99-2207	Syatteityvis	Fluvial sand; depth 1.5 m	75 ± 6	109 ± 6	24	1.46 ± 0.08	27
002529	99-2209	Syatteityvis	Fluvial sand; depth 6.3 m	77 ± 6	141 ± 6	24	1.83 ± 0.10	25

Results

Lake Kormovoye

Lake Kormovoye (66°44.5′N, 56°42.5′E, 94 m a.s.l.; unofficial name) is a small (ca. 0.3 km^2), elongated lake ≤5.9 m deep (Fig. 2). The lake lies just inside and parallel to the Laya-Adzva Moraine, a large lobe-shaped push moraine. This moraine protrudes further south of, and is subsequently cut by, the hummocky landscape of the Harbei Moraine (Astakhov *et al.*, 1999) (Fig. 1). The Laya-Adzva Moraine has not been dated, but owing to its relatively fresh appearance it is thought to be of post-Eemian age. Lake Komi shorelines, OSL dated to about 90 ka, are mapped inside the moraine (Mangerud *et al.*, 1999, 2001) and therefore provide a minimum age. The Laya-Adzva Moraine probably formed during an early phase of the 90 ka ice advance (Mangerud *et al.*, 1999). The catchment area of the lake is ca. 5 km^2 and drainage into the lake is via a creek in the western end and additional sheet flow during spring. Today the lake is surrounded by an open spruce forest, and lies outside the zone of permafrost (Fig. 1).

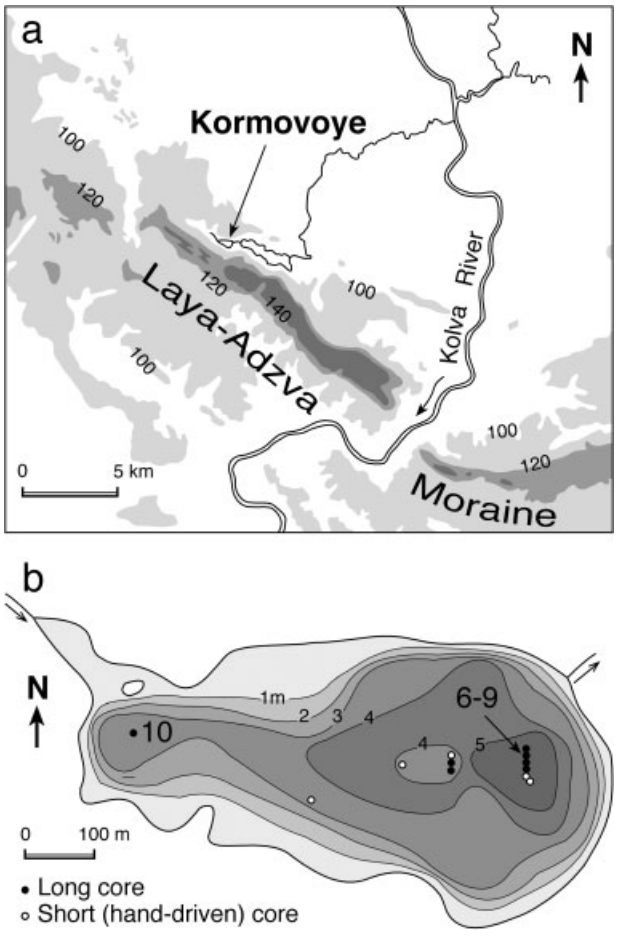

Figure 2 (a) Location of Lake Kormovoye just within the Laya-Adzva Moraine. Higher areas are darker. Some altitudes are given in m a.s.l. on some contours. (b) Bathymetric map of Lake Kormovoye with 1-m contour intervals. Only cores 6, 7, 8 and 9 from the deepest basin and core 10 near the inlet creek are discussed in the text

Three main lithostratigraphical units, labelled A–C from the base, have been recognised in the cores (Fig. 3 and Table 3): unit A is a diamicton, unit B clayey silt and unit C is gyttja. In Lake Kormovoye we cored only down to the diamicton as we at that time interpreted it as a till from the last glaciation. We recovered four cores (6–9) in a north–south transect at 5.6 m water depth in the deepest basin (Fig. 2). Even though the distance between each core was only 2–3.5 m the diamicton appears at different depths and there are major variations in the silt unit as well (Fig. 3 and Table 3). The upper gyttja (1.3–1.5 m thick) is similar in all cores. Core 10 was sampled at 3.1 m depth, close to the inflow in the western part of the lake. Several other cores from the lake exhibit similar stratigraphy, but they were not analysed in detail.

Unit A—diamicton

The lowermost unit is a clayey, matrix-supported diamicton, weakly stratified with some sorted layers. The thickness of this unit is unknown. In core 9 the diamicton is below 7.6 m, whereas it is found at shallower depths in cores 6–8 (Fig. 3 and Table 3). In core 10 there are two diamicton beds. The diamictons are in all the cores interpreted as sediment gravity flow deposits, based mainly on the stratification, the repetition in core 10, and the different ages of the overlying sediments (see below).

Unit B—silt

Unit B, up to 6.3 m thick, consists of laminated to massive clayey silt with a sharp lower contact with unit A (Fig. 3 and

Table 3 Lithostratigraphical description of the sediment sequence from Lake Kormovoye

Unit	Core number: sediment depth (m)	Sediment description, unit characterisation
C2	6: 0.00–1.00; 7: 1.00–1.18; 8: 1.00–1.13; 9: 0.50–1.10; 10: 0.50–1.98	Soft and partly elastic, fine silt-gyttja, laminated except in its uppermost 30 cm where it is massive. Very dark greyish brown to dark olive-grey colour, the silt-gyttja contains scattered macrofossils, getting sparser and smaller upward. Sharp lower boundary. In core 10 it is interbedded with layers of coarse detritus gyttja. LOI: 6–17%; water content: 58–76%; MS: $<4\ 10^{-5}$ SI
C1	6: 1.00–1.13; 7: 1.18–1.26; 8: 1.13–1.26; 9: 1.10–1.25	Very dark brown, coarse-detritus gyttja to silt-gyttja, partly laminated. The organic matter coarsens upwards, and includes a lot of twigs, leaves, needles, etc. Gradual lower boundary. LOI: 10–26% water content: 50–70%
B7	10: 1.98–3.34;10: 4.50–5.05	Dark olive-grey, laminated to massive silty clay with scattered pebbles and cobbles, coarsening upwards to clayey silt with less amount of scattered gravel. Plant macrofossils present above 3.1 m. LOI: 2.1–3.5%
B6	6: 1.13–1.94; 7: 1.26–1.74; 8: 1.26–1.31; 9: 1.25–2.05	Dark grey to olive-grey laminated silt, changing upwards to massive clayey silt. Plant macrofossils are increasing upwards. LOI: 1.5–8% water content: 20–32%
B5	8: 1.31–2.00?; 9: 2.05–2.22	Laminated (and partly massive?) silt, of olive-grey colour with several organic rich laminae. This unit is characterised by very high values of *Betula* pollen. Sharp boundaries, hiati above and below seen by the pollen analysis. LOI: 3–10%; water content: 22–30%
B4	8: 2.00?–5.32	Very dark greyish brown and dark grey, clayey silt to silt-gyttja with coarse detritus organic layers and clasts of organic matter, including a 30-cm-thick organic-rich bed with twigs. The organic bed has high LOI values (20–31%), elsewhere 4–13%. Water content: 19–34%, organic clast: 43–50%
B3	6: 1.94–3.00; 7: 1.74–3.10; 9: 2.22–3.95	Dark grey to olive-grey, laminated clayey silt with some brownish, organic laminae. The organic content is slightly higher than unit B2 (LOI 2–5%) and considerably higher in the organic laminae (LOI up to 8%). Some few scattered plant macrofossils. Gradual lower boundary set at the first occurence of organic laminae. Water content: 17–30%
B2	6: 3.00–4.80; 7: 3.10–4.33; 9: 3.95–5.56	Dark grey and olive-grey, laminated clayey silt with low organic content; few and small plant macrofossils are found scattered. Gradual lower boundary towards unit B1, sharp lower boundary towards unit A. LOI: 2–4% water content: 13–23%
B1	9: 5.56–7.58	Dark grey, laminated clayey silt with low organic content; no visible plant macrofossils. Sharp lower contact with unit A. LOI: 2–3%; water content: 15–20%; MS: $<12\ 10^{-5}$ SI in whole unit B except the lowermost ca. 40 cm of unit B1 in core 9
A	6: 4.80–5.00; 7: 4.33–5.50; 8: 5.32–5.40; 9: 7.58–8.50; 10: 3.34–4.50; 10: 5.05–7.05	Very dark grey, matrix-supported, clayey diamicton, consisting of silty, sandy clay with scattered pebbles and cobbles. Massive to weakly stratified with some sorted layers. LOI: 2–4%; water content: 15–20%; MS: $<10^{-5}$ SI

Table 3). This unit includes some deformation structures including convex folding of laminae confined to the width of the cores and laminae being blurred along the mid-axis of the cores, interpreted to be caused by the coring operation. In the deepest basin, unit B is divided into six subunits (B1–B6) based mainly on lithology and partly on pollen assemblage and chronology. In core 10 a subunit is labelled B7. Thirteen ^{14}C dates yielding ages 11 730 to 3900 yr BP were obtained from cores 7–9 (Table 1).

Unit B1 is found only in the lower part of core 9. It consists of laminated clayey silt with low organic content and no visible plant macrofossils. It is considered to be the oldest part of unit B.

Unit B2 is similar to B1, except that few and small plant macrofossils are found scattered throughout the unit. It overlies B1 in core 9. A twig at the base of unit B2 in core 9 has been dated to 11.6 kyr BP. Pollen zone K-1 includes units B1 and B2, and is dominated by grasses and herbs such as *Artemisia* and Brassicaceae (Fig. 4). Redeposited microfossils including pre-Quaternary pollen are frequent. *Betula*, probably consisting of both *in situ* dwarf birch and reworked grains, constitutes 10–20% of the pollen.

Unit B3 differs from B2 by the occurrence of brownish, organic laminae and a slightly higher organic content. The three organic laminae in cores 6 and 7 (Fig. 3) are interpreted to correlate with each other, and possibly also with the three lowermost laminae in core 9. The lower organic laminae in cores 7 and 9 have been dated to 11.0–11.7 kyr BP. Pollen zone K-2 is dominated by *Artemisia* and grasses, but also contains distinct amounts of Cyperaceae, *Salix* and *Dryas*, indicating slightly moister tundra vegetation, consistent with the higher organic content in unit B3 than B2.

Unit B4 is found only in core 8. It is distinctly different from the entire unit B in cores 6, 7 and 9 owing to its brownish colour. It consists of 3.4 m of clayey silt to silt-gyttja with organic layers and clasts, giving high LOI values. Several dates from the whole unit suggest an age of ca. 9.9 kyr BP, indicating that unit B4 stratigraphically should be between units B3 and B5 in core 9. Note that unit B4 in core 8 is deposited directly on the diamicton (unit A).

Unit B5 in core 9 is laminated silt, but mainly identified as pollen zone K-3 characterised by very high values of *Betula* (Fig. 4), and dated to 9.0–9.6 kyr BP. The boundaries of pollen zone K-3 are abrupt and probably represent hiati, in which the lower hiatus constitutes around 1000 yr.

Lithologically the sediments in the lower part of unit B6 are similar to B5, but upwards there is a change to massive clayey silt. The ^{14}C dates yielded an age of ca. 4.1 kyr BP, so there is a major hiatus of ca. 5000 yr between B5 and B6. The pollen content in B6, showing high *Betula* and increase of *Picea* and *Filipendula*, suggests a climate as warm as at the present.

The laminated silt in core 10, collected near the inlet, cannot be correlated directly with the units in the other cores. Unit B7 is found between and above the diamictic layers, and consists of laminated to massive silty clay with scattered pebbles and cobbles coarsening upwards to clayey silt with less scattered gravel. Both depositional processes and age (although not dated) probably can be compared with units B1 and B2 in the deeper part of the lake, as B7 below 3.1 m contains no visible plant macrofossils, similar to B1.

The laminated to massive fine-grained sediments of unit B are attributed to suspension settling in a small lake, where the coarser grain size in core 10 is attributable to proximity

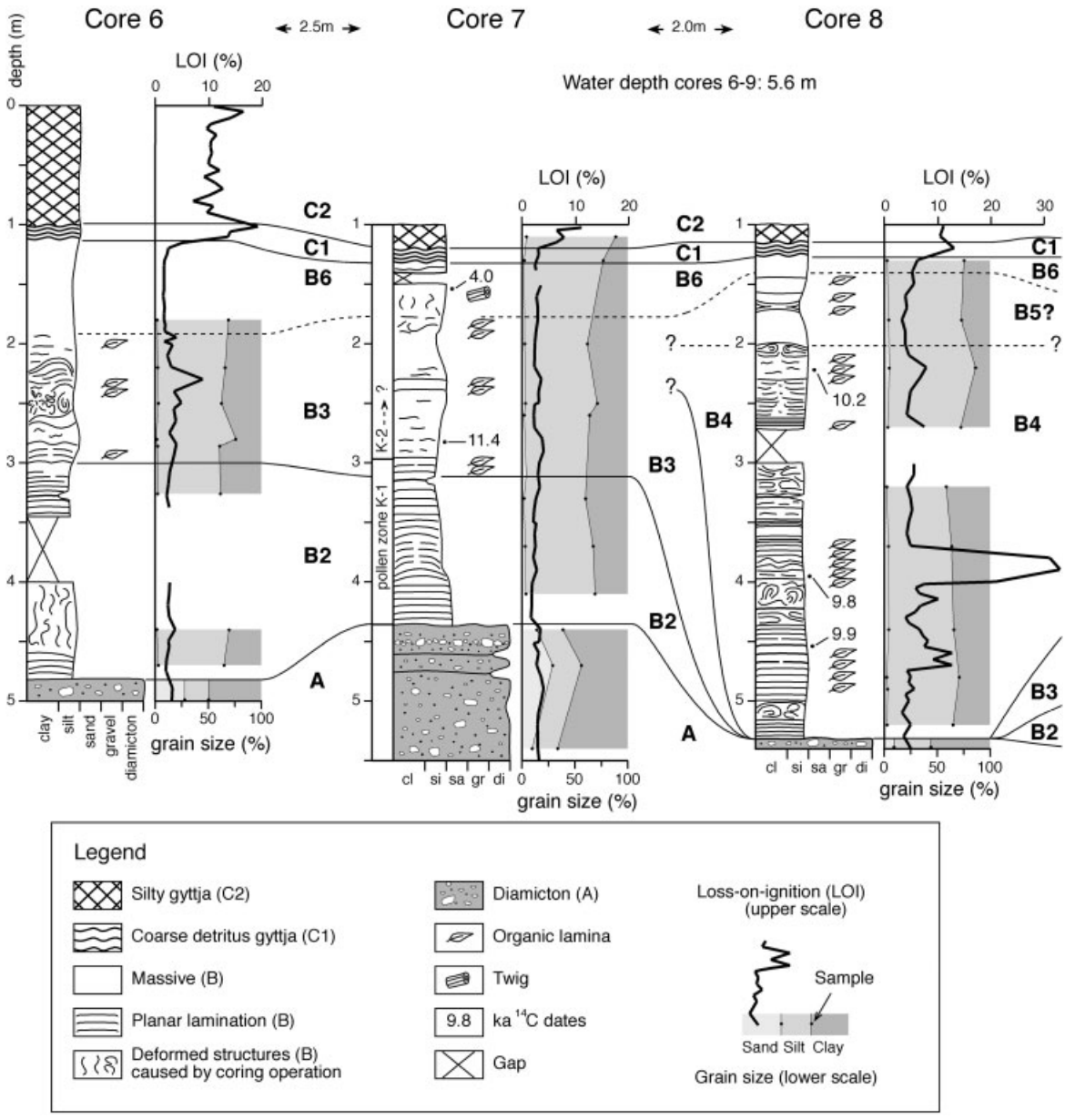

Figure 3 Logs of cores 6, 7, 8, 9 and 10 from Lake Kormovoye. All are plotted on the same depth scale, measured from the lake floor. Distances between the cores and water depth are given on the top. The lithostratigraphical units are indicated by letters (A, B1–B7, C1–C2) and correlation between the cores with solid lines. Dashed lines indicate tentative correlations. The pollen zones (Fig. 4) are marked along core 9 and part of core 7

to the inflow of the creek. Lateral variations over short distances and occurrence of several hiati suggest aperiodic and/or spatially discrete sedimentation of unit B during the late-glacial and Holocene. The discrepancy between the ^{14}C dates from units B2 and B3 indicating an Allerød age and the pollen composition (Y-1 and Y-2) indicating cold steppe and tundra vegetation, suggest that older organic matter was washed into the lake during the Younger Dryas stadial. Reworked organic matter yields so errantly old ^{14}C dates, thus yielding maximum dates, which is a common dating problem in permafrost areas, where organic matter often is well preserved (e.g. Nelson *et al.*, 1988; Murton, 1996). Reversed dates in B4 and B5, the former also including organic clasts, suggest that older organic matter was also washed into the lake during the early Holocene. Nevertheless, as the dated units become successively younger upwards there is probably not too great a discrepancy between the actual age and the ^{14}C dates of each unit.

Unit C—gyttja

Unit C1 is a layer of coarse-detritus gyttja 10–20 cm thick with a gradational lower boundary and a high LOI, found in all cores in the basin (Fig. 3 and Table 3). The depths are also similar, indicating that the lateral differences seen in unit B have been eliminated before deposition of unit C. Three dates yielded consistent ages from 4.1 to 4.3 ka (Table 1). Pollen zone K-5 is identified in unit C1 and C2, and is dominated by further increase of tree pollen (Fig. 4). The organic matter in C1 coarsens upwards and we assume the gyttja was deposited in a small lake that gradually became shallower. The fact that unit C1 is missing in core 10 may suggest that the site of this core was exposed at this time.

Unit C2 consists of soft, laminated fine silt-gyttja, which is massive in its uppermost 30 cm. It contains scattered macrofossils, sparser and smaller upwards. A sharp lower boundary indicates a shift in depositional conditions from the shallow water

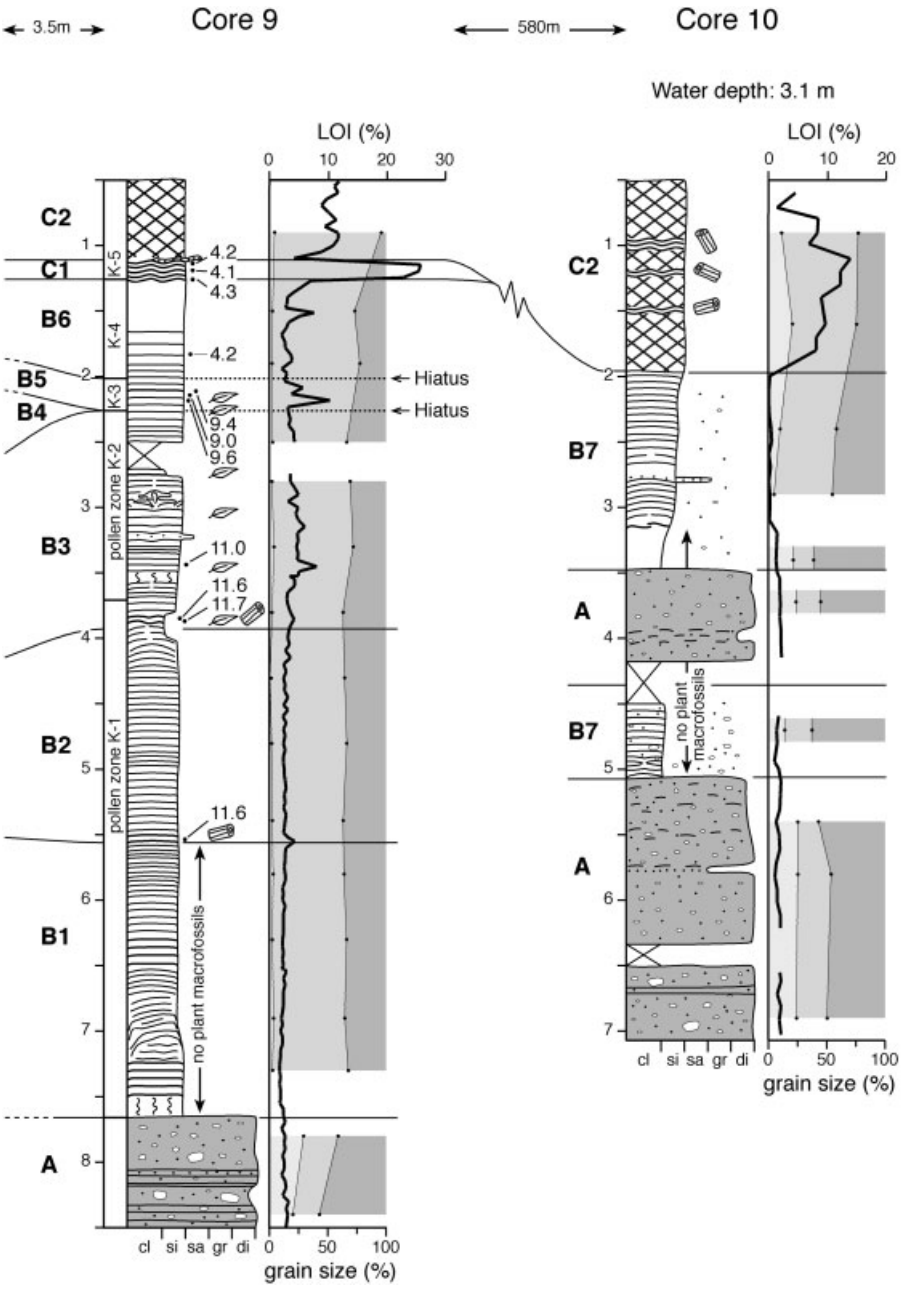

Figure 3 Continued

in C1 to a deeper lake. The transition to massive gyttja at the top suggests another shallowing episode.

Lake development

Lake Kormovoye is located within a depression topographically controlled by the push moraine ridges of the Laya-Adzva Moraine (Fig. 2). We find it most likely that the lake was formed when buried glacier ice melted.

The lowermost unit A is interpreted as sediment gravity flow deposits, most likely redeposited ablation till (flow till) flowing from the top of the buried ice. In core 10 the two separate diamictic layers suggest that such mass flow occurred also after the lake was established. The first 'normal lake' sedimentation is represented by unit B1, found only in core 9. One can only speculate if B1 is found below unit A in cores 6–8, and thus that diamicton A was deposited as a sediment gravity flow at a time when B1 and B2 were deposited at core site 9, or if a lake depression first existed only at core site 9.

Unit B is interpreted as lacustrine silt settled from suspension. The ^{14}C dates and pollen analyses indicate that there are several hiati present and that units B1–B3 were continuously deposited during the Younger Dryas stadial, whereas units B4 and B5 are of early Holocene age and B6 is from the middle Holocene. The most striking feature of the cores from Lake Kormovoye is the prominent lateral changes in sediment sequences within extremely short distances. For example, in core 9 the laminated silt of units B2 and B3 are found at a depth of 2.2–5.5 m, whereas a different and much younger unit B4 is found at the same depth in core 8, which is located only 3.5 m away from core 9. Moving another 2.5 m to core 7, B4 is again replaced by B2 and B3. This architecture cannot possibly have resulted from deposition in a 'normal lake' with a stable lake floor but rather on an unevenly

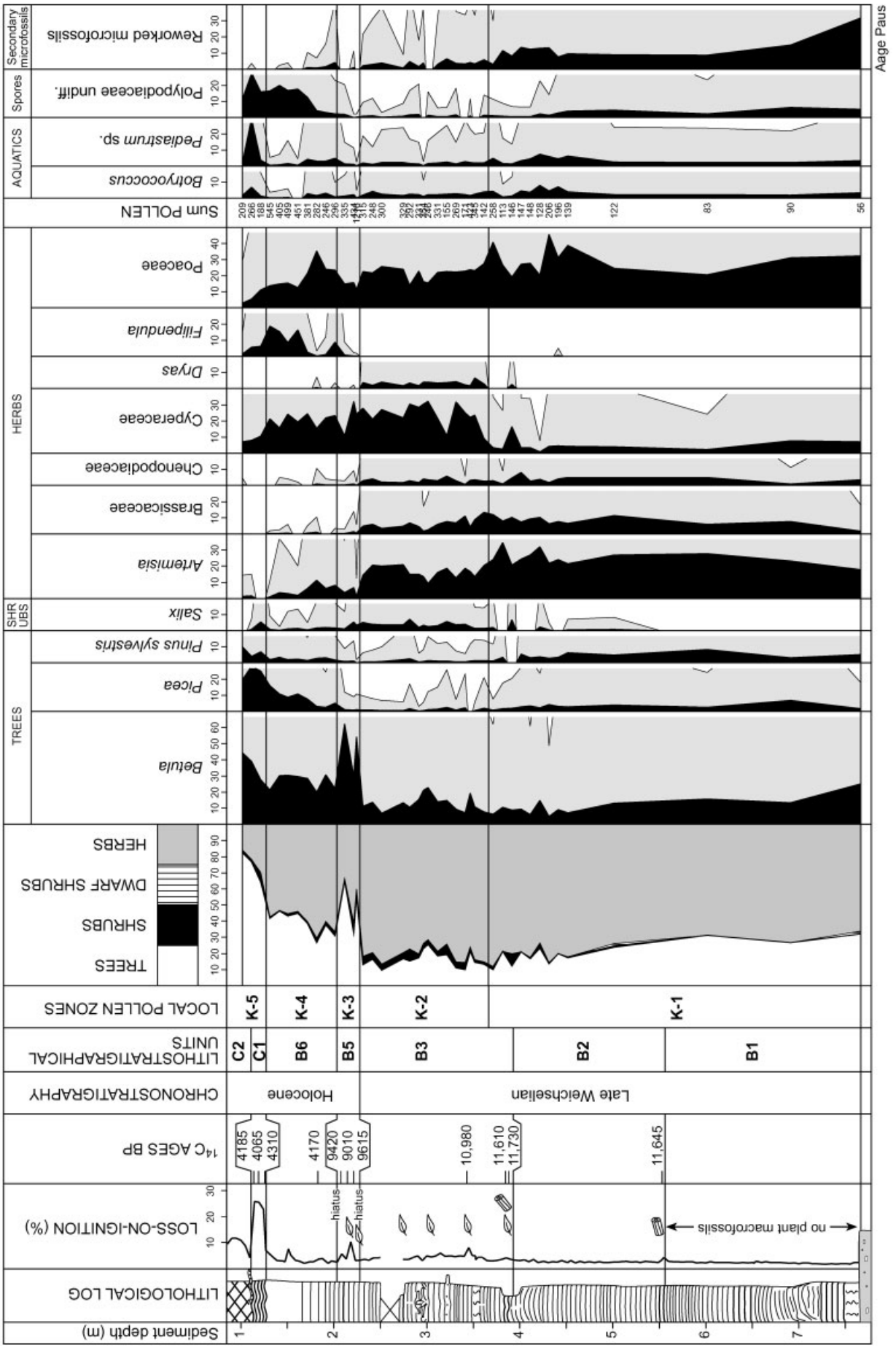

Figure 4 Pollen percentage diagram from core 9, Lake Kormovoye plotted versus sediment depth. The legend for the lithological log is given in Fig. 3

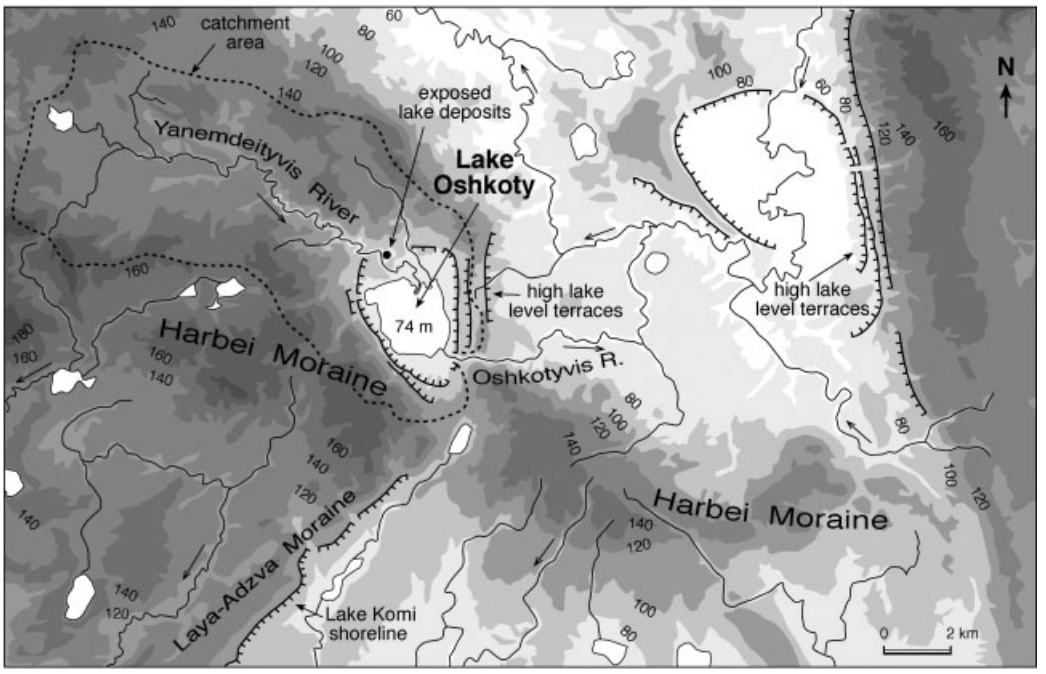

Figure 5 Location of Lake Oshkoty inside the Harbei Moraine. The catchment area and shorelines of former high lake-levels are shown. Contour intervals are given in m a.s.l

subsiding lake floor. The most likely explanation is that the sediments were deposited on buried glacier ice, and partly redeposited from higher to lower elevated areas as parts of the underlying ice melted.

There was probably more or less continuous subsidence at the individual sites. For example, when B2 was deposited, core sites 7 and 9 were subsiding, and thus laminated lacustrine sediments were continuously deposited in a lake maintaining its depth, whereas core site 8 was probably above lake-level or at very shallow water depths undergoing non-deposition or erosion at this time. At the onset of deposition of B4 core site 8 started to subside, whereas core sites 7 and 9 became elevated and possible exposed, and sediments from these sites probably were redeposited into site 8 in the early Holocene. This probably corresponds to the hiatus between units B3 and B5 in core 9. Sedimentation continued with deposition of unit B5 in core site 9, and possibly also in other places, later in the early Holocene. This sedimentation model with differential subsidence implies relative vertical movements either along faults or by ductile deformation, which must have occurred in between the coring sites as we have no observation of either in the cores.

The lake floor in the main basin (cores 6–9) was more or less even at the onset of unit B6, implying that buried ice had vanished by 9 ka, more or less at the same time as the northward shift in permafrost distribution (Baulin *et al.*, 1984). A lowering of the lake-level, allowing erosion and non-deposition, was probably responsible for the 5000-yr long hiatus seen between units B5 and B6 in core 9. Similar decrease in lake-level is recorded in many Russian lakes in the early to middle Holocene (e.g. Davydova *et al.*, 1992). As deposition continued in the middle Holocene, the lake became shallower before its level rose once again and eutrophication of the lake took place with deposition of gyttja C from ca. 4 ka to the present. The Holocene lake-level fluctuations seen in Lake Kormovoye probably were controlled by fluctuations of the groundwater level, ultimately affected by the local evaporation–precipitation rate. Lowering and rising of the outlet as a result of downcutting or peat aggradation, respectively, also may have caused some lake-level fluctuations.

Lake Oshkoty

Lake Oshkoty (67°42′N, 57°15′E, 74 m a.s.l.) is situated just inside the Harbei Moraine (Astakhov *et al.*, 1999), dated to 90–80 ka (Mangerud *et al.*, 2001, in press), and located 250 km to the north of Kormovoye (Figs 1 and 5). It is located in an isolated patch of swampy flatland (ca. 55 km^2) in the northern tundra zone, just within the zone of continuous

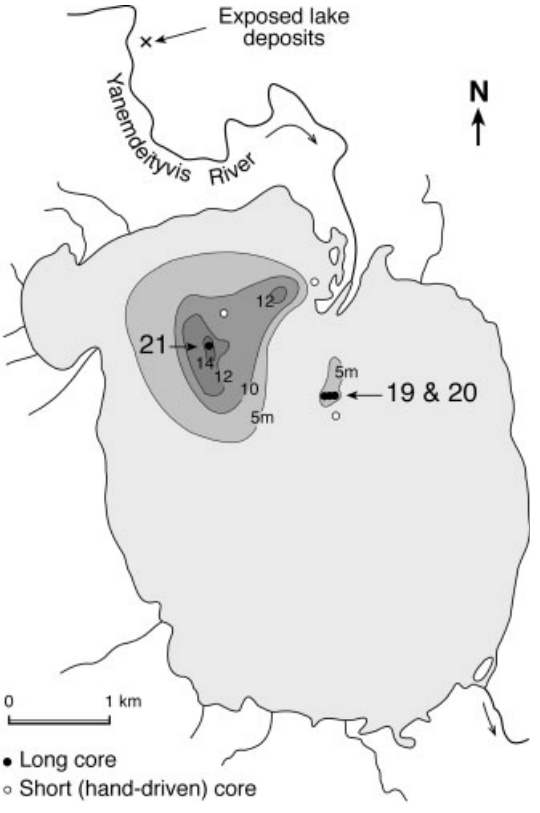

Figure 6 Bathymetric map of Lake Oshkoty. Note the uneven contour intervals. Only the numbered cores are discussed

permafrost (Brown *et al.*, 1997). The lake occupies 16 km^2 and has two small basins with maximum depths of 14.2 m and 7.3 m respectively, but most of the lake is less than 5 m deep (Fig. 6). The total catchment area of the lake is 370 km^2. Yanemdeityvis is the only large river entering the lake and it forms a sandy finger delta. There are also several small creeks draining into the lake. The outlet-river Oshkotyvis runs through a 20–30 m deep, narrow valley cut into the morainic landscape. Several terraces surrounding the lake show that it has been larger; the most pronounced terrace is at 80–90 m a.s.l. Traces of other former large lakes are seen further east in this area (Fig. 5).

Three long cores from the lake are described here, core 21 from 14.1 m depth in the deepest basin and cores 19 and 20 sampled 2–3 m apart at 7 m water depth in the shallower basin ca. 1.3 km to the east (Fig. 6). The sediments are subdivided into three units: unit D is a diamicton in the lower part of the sequence, unit E consists of sand and gravel, and the upper unit F is a silty clay (Fig. 7 and Table 4). In addition, a description of exposed lake sediments along the River Yanemdeityvis, located 1.7 km north of Lake Oshkoty (Figs 6 and 8) is included in order to define former shorelines (terraces).

Unit D—diamicton

Unit D is a partly stratified, not overconsolidated, matrix-supported clayey diamicton with a recovery of 16 m in core 21. Coring so deep into the diamicton was a result of the experience in Lake Kormovoye. We wanted to test whether there were older lacustrine sediments buried beneath the diamicton. Unit D is interbedded with layers of laminated clay, sand and gravelly silt, some layers containing discontinuous and deformed laminae including structures such as small-scale folding, faulting and load casts not confined to the middle of the core. At least one of the diamictic beds exhibits reverse grading (Fig. 7 and Table 4).

Unit D is interpreted as sediment gravity flow deposits (flow till) based on stratification, reverse grading and the many diamictic beds in the upper part of the unit. The diamictic sediments probably originate from a till laid down by the same ice advance that deposited the Harbei Moraine a few kilometres to the south (Fig. 5). The sand and clay layers interbedded with the diamicton are interpreted as being deposited from suspension in the lake, and the deformation of these layers is probably caused by loading and movement during emplacement of the overlying diamictic beds. However, it cannot be ruled out that the lower part of unit D was deposited as a basal till.

Unit E—sand and gravel

Unit E consists of interbedded layers of sand, sandy gravel and gravelly silt. A couple of organic laminae (Fig. 7 and Table 4) are also found, yielding radiocarbon ages of 12.3 ka in core 19 and 11.4 ka in core 21 (Table 1). We correlate the high magnetic susceptibility values at 12.6 and 15.6 m in core 20 and 21 respectively.

The large variation of grain size and degree of sorting indicate different depositional processes. The coarse layers of sand and gravel are interpreted as different types of sediment gravity flow and slump deposits originating from delta or shore sediments surrounding the lake, whereas the laminated silt is interpreted as being deposited from fall-out in the lake. Outsized clasts in the silt probably originate from river-ice floating into the lake. The coarse sediments in unit E indicate a smaller lake and thus lower lake-level than at present.

Unit F—clay

The uppermost unit is between 10.2 and 13.2 m thick and consists of sticky and vesicular laminated silty clay to gyttja-clay with some black sulphur laminae and stains. Individual laminae of coarser silt and fine sand are found scattered throughout the cores (Fig. 7 and Table 4). There are a few scattered, small macrofossils and thin organic horizons. In core 20 some fining upwards layers and small-scale synsedimentary normal faults have been recognised (Fig. 7).

Unit F is interpreted mainly as deposition from fall-out in a lake with periodically anoxic bottom water. The coarser silt and fine-sand laminae as well as the normal graded laminae are interpreted as mass-flow deposits. The coarser lowermost part was probably deposited in shallower water, where the sediments have been reworked by waves causing different dip directions of the laminae.

Exposed lacustrine sediments

A 6-m-high section through a terrace (84 m a.s.l. and 10 m above the lake-level) along the River Yanemdeityvis (Fig. 5), north of Lake Oshkoty, shows planar parallel laminated silt in its lower part (Fig. 8). Upwards, the silt is interbedded with sand, occasionally with wave ripples. Above the silt there is a gravel bed with subhorizontal sand layers, which is overlain by laminated silty sand fining upwards to silt. The upper part of the section is a peat including logs up to 18 cm in diameter and dissected by ice-wedge casts. Two radiocarbon dates of 10.6 and 9.4 ka were obtained from the lower lacustrine silt and sand, and a log from the overlying peat was dated to 6.6 ka (Table 1).

The lower silt and sand beds are interpreted as lacustrine sediments and the gravel bed as shore sediment deposited in Lake Oshkoty. As the gravel bed lies at ca. 80 m a.s.l., it correlates with the 80–90 m terrace surrounding Lake Oshkoty (Fig. 5), thus showing that the terraces are former shorelines. The lower silt and sand is correlated with unit F in the lake. The coarsening upward sequence reflects shallower lake-level ending with deposition of terrestrial floodplain and slumped sediments with peat forming at the top.

Lake development

Owing to the size of the lake depression and the location just inside the Harbei Moraine (Figs 5 and 6), Lake Oshkoty is interpreted as formed by melting of buried glacier ice. Lake sedimentation seems to have started at 11–12 ka, probably owing to subsiding of the lake floor as the ice melted. The many sediment gravity flow deposits in units D and E indicate that the sediment accumulated on the floor of a lake surrounded by unstable soil, probably owing to melting of the permafrost. Sedimentation by fall-out from the water column took place in between the flow events. The coarser deposits in unit E, compared with the lacustrine sediments between the diamictic layers in unit D, indicate a falling lake-level, probably caused by lowering of the threshold. Later, the laminated, fine-grained sediments of unit F indicate a more stable soil condition and deposition in deeper water from suspension and occasional density currents. This relative lake-level rise from unit E to F is probably the result of increased melting of underlying dead ice, causing subsidence of the lake floor.

Unit F, although not dated, is inferred to be Holocene. The early Holocene lacustrine sediments that were recorded from the exposed section north of the lake probably correlate with the lower parts of unit F and also with the terrace at

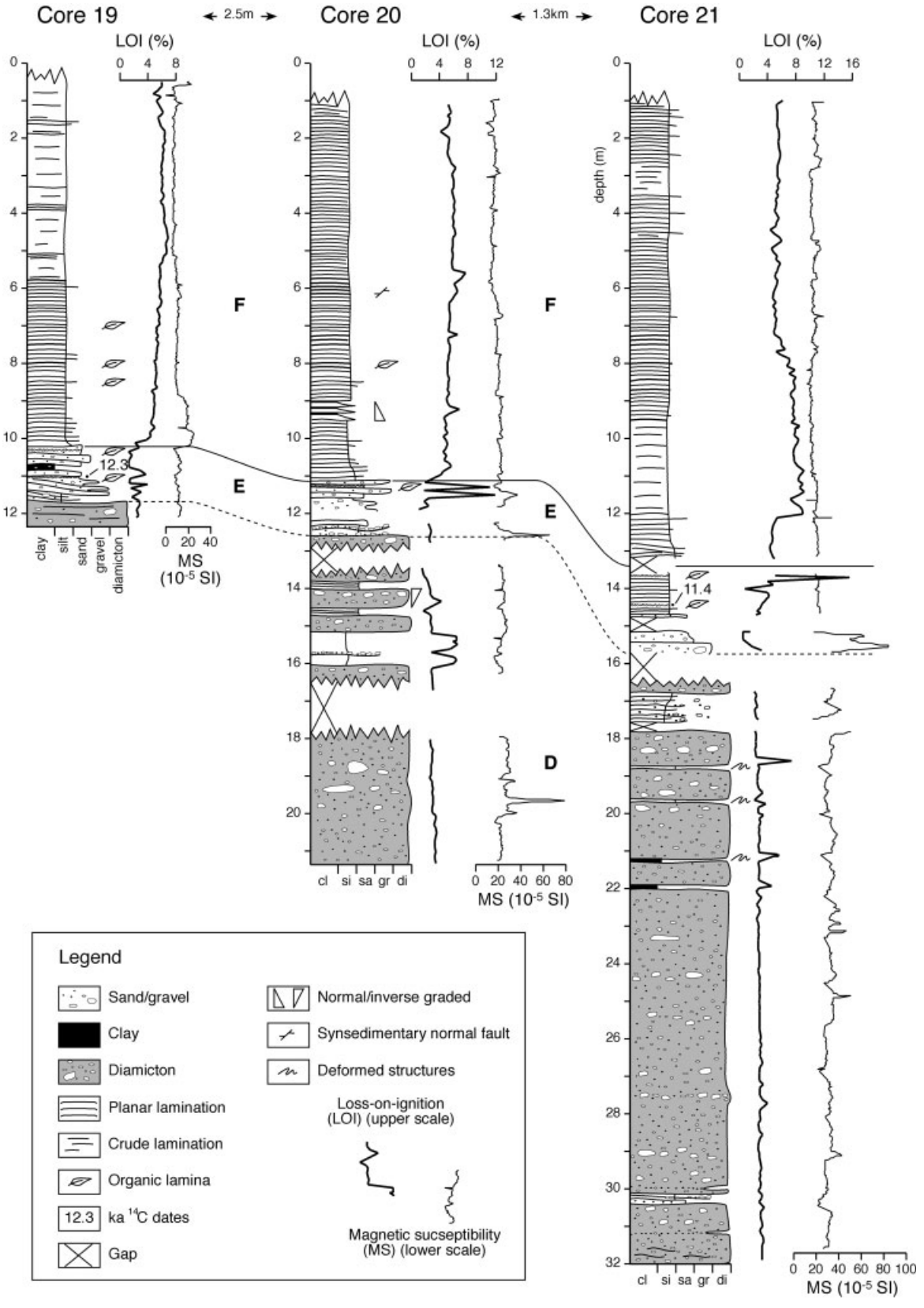

Figure 7 Logs of cores 19, 20 and 21 from Lake Oshkoty. All logs are plotted on the same depth scale, measured from the lake floor, which is at water depth of 7.0 m for cores 19 and 20 and 14.1 for core 21. The lithostratigraphical units are shown with letters (D, E, F) and correlation between the cores with solid lines. Dashed lines indicate tentative correlations. The deformed structures consist of small-scale folding, faulting and load casts

80–90 m a.s.l. surrounding Lake Oshkoty. The dates from the exposed section show that the lake-level was falling at the very beginning of the Holocene and that the threshold was below 80 m a.s.l. sometime after 9.4 ka. The tree trunks show that the area was forested, corresponding with the period between 9000 and 4000 ^{14}C yr BP when the northern treeline reached the Barents Sea coast (Khotinskiy, 1984; Kremenetski *et al.*, 1998; MacDonald *et al.*, 2000). We find it probable that the formation of the ice-wedges, which post-date the peat, started at the same time as the deforestation around 4 ka, during the

Table 4 Lithostratigraphical description of the sediment sequence from Lake Oshkoty

Unit	Core number: sediment depth (m)	Sediment description, unit characterisation
F	19: 0.40–10.10; 20: 1.00–11.10; 21: 1.00–13.20	Laminated silty clay to gyttja-clay with some more massive intervals, colour is dark grey to very dark grey, except in the uppermost few metres being olive grey. The silty clay has black FeS laminae and stains, and is sticky and vesicular. It contains only a few scattered, small macrofossils and thin organic laminae, while individual laminae of coarser silt and fine sand are found scattered throughout the unit. In core 20 some fining upward layers and small-scale synsedimentary faults have been recognised. LOI: 4–10%; water content: 30–65%; MS: 5–25 10^{-5} SI
E	19: 10.10–11.60; 20: 11.10–12.50; 21: 13.60–15.70	Interbedded layers of sandy gravel, pale red, olive and olive grey sand and dark grey, gravelly silt as well as some organis laminae. The content of organic matter and MS are highly variable. LOI: 0.5–15.6%; water content is 8–45%; MS: 8–85 10^{-5} SI
D	19: 11.60–12.15; 20: 12.50–21.40; 21: 15.70–31.70	Dark grey, matrix-supported, clayey diamicton, not overconsolidated. It is at least 16 m thick in core 21, and is partly stratified where one of the diamictic beds exhibit reverse grading. In the lower part of core 21, the diamicton is slightly sandier, and is interbedded with layers of light grey sand and gravelly silt. In its upper part, unit D is interbedded with layers of very dark grey, laminated clay and sand, where some of the laminae are discontinuous and deformed including small-scale folding, faulting and load cast not confined to the middle of the core. Most of these sorted layers are found in the upper part of the unit. Some of the layers contain discontinuous and deformed laminae including small-scale folding, faulting and load cast not confined to the middle of the core LOI: 1.5–4.0%, the sorted layers up to 7.4% water content: 14–22%, in sorted layers up to 36% MS: 10–40 10^{-5} SI with peak values of 50 and 80 10^{-5} SI in core 20 and 21 respectively

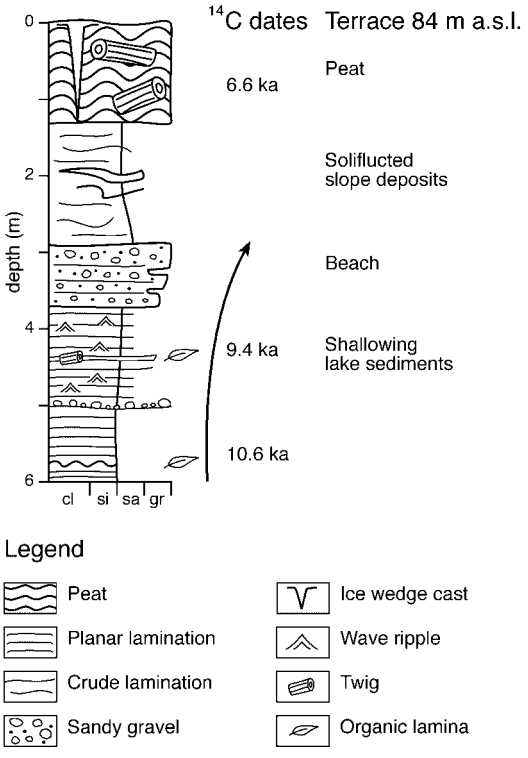

Figure 8 Log of section in exposed lake sediments on River Yanemdeityvis, north of Lake Oshkoty (Fig. 6). The arrow indicates coarsening upwards sequence

late Holocene, cooling with subsequent southward shift in permafrost distribution (Baulin *et al.*, 1984; Väliranta *et al.*, 2003).

Other localities

Lake Lyadhei-To area

Lyadhei-To (68°15′N, 65°48′E, 152 m a.s.l.) is a lake located at the northern foot of the Polar Ural Mountains proximal to the Halmer Moraine (Astakhov *et al.*, 1999) (Figs 1 and 9). The investigation of this site was done in collaboration with the Alfred-Wegener Institute, Potsdam, Germany, who collected and described cores from this lake. We (M. Henriksen and co-worker O. Maslenikova, St Petersburg University) mapped the area and described sections around Lake Lyadhei-To. The lake basin was selected by us because of its location close to bedrock. We expected that the existence of any dead ice at this site should have melted out much earlier than within the sediment basin of the Pechora Lowland, thus yielding a much longer lake record.

At a site southwest of the lake, glacial striae on exposed bedrock showed ice flow from the northeast, supporting the conclusion that the last ice flow across the area was from the Kara Sea and up-valley in the northern Urals (Astakhov *et al.*, 1996). A hummocky landscape surrounds the lake (Fig. 9), probably formed during disintegration of the shelf-centred ice-sheet. The lake is 26 m deep (Wischer *et al.*, 2001) but it is unclear how much is a result of overdeepening of the bedrock. Samples from kames of glaciofluvial ripple laminated fine sand, occasionally draped by mud, were OSL-dated to 87, 114, 120 and 125 ka (Table 2). Considering that kame sediments may be incompletely bleached, we consider the youngest date as most reliable, supporting an age for the Halmer Moraine of about 90 ka (Mangerud *et al.*, 1999, 2001).

Cores from Lake Lyadhei-To reveal diamicton in its lowermost part overlain by 7 m of lacustrine clayey and silty gyttja. We expected that the basal layers of this lake were laid down shortly after the deglaciation around 90–80 ka. However, in the basal part terrestrial plant remains are ^{14}C dated to the Weichselian–Holocene transition around 9.5 kyr BP (Wischer *et al.*, 2001). It therefore seems clear that this basin also was filled by glacier ice until the early Holocene.

Syatteityvis

Fluvial sediments along the River Syatteityvis (67°27′N, 62°38′E, 90 m a.s.l.) are located inside the Harbei Moraine and thus post-date the last ice advance in this area (Figs 1 and 10). Samples of fluvial fine sand from a section 15 m high along the river were OSL dated to 75 and 77 ka (Table 2), again supporting deglaciation of the area soon after 90 ka.

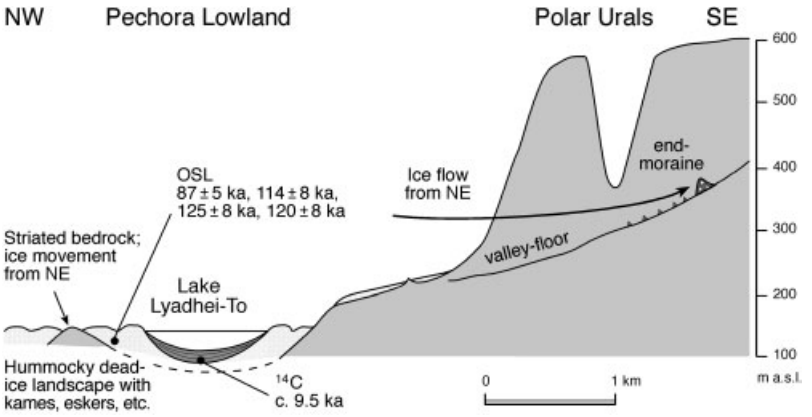

Figure 9 Schematic cross-section through the northern tip of the Ural Mountains. Note that glacial striae, erratics and the form of the end-moraines show that the last ice flow was from the Kara Sea and up-valley in the mountains. Basal ^{14}C date of lake sediments (Wischer *et al.*, 2001) and OSL dates from glaciofluvial sand are indicated.

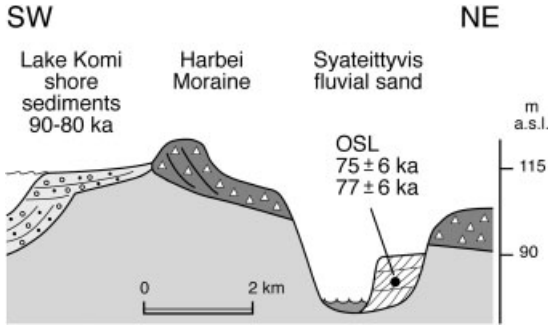

Figure 10 Schematic location of the Syateittyvis fluvial section cutting into the Early Weichselian Harbei morainic landscape. The OSL dates from the fluvial section are shown as well as the mean of many OSL dates of Lake Komi shore sediments (Mangerud *et al.*, 2001; in press)

Discussion

Formation of the lakes

The numerous lakes within the hummocky landscape of the northern Pechora Lowland derive, according to Astakhov *et al.* (1999), from melting of stagnant glacier ice and degradation of the Pleistocene permafrost. Owing to their size and because the basins relatively deep, the Kormovoye, Oshkoty and Lyadhei-To lakes are interpreted to result from melted massive ice. Although the ice could have been intrasedimental ice, i.e. frozen ground water (cf. Mackay and Dallimore, 1992), we believe it was more likely to be buried glacier ice, because the lake basins are so deep and located proximal to moraines. Further indications of glacial thermokarst are that Lake Kormovoye is topographically controlled by morainic ridges, and that Lyadhei-To is surrounded by kames.

A similar two-stage sedimentation as that described from thermokarst lake basins in Arctic Canada (Rampton, 1973, 1988; Murton, 1996) is also identified in this study. Melting of buried glacier ice, ground subsidence and depositional processes were closely related in the first stage of dead-ice lake evolution (Fig. 11). As the dead ice started to melt the debris enclosed in it was deposited as ablation till. In places with thick masses of buried glacier ice, depressions developed and the surrounding sediments became unstable. This caused slumping and flowing of sediments into the lake where such deposits became interbedded with lacustrine mud. These mass flow layers are found mainly in the lower parts of the sequences, indicating that the initial stage was followed by stabilisation when most of the buried ice was melted and a denser vegetation cover established. Sedimentation from suspension dominates the younger part of the lake sequences (Fig. 11) with occasional deposition from density currents and debris flows.

However, even during the second stage dominated by normal lake sedimentation, buried dead ice must have existed.

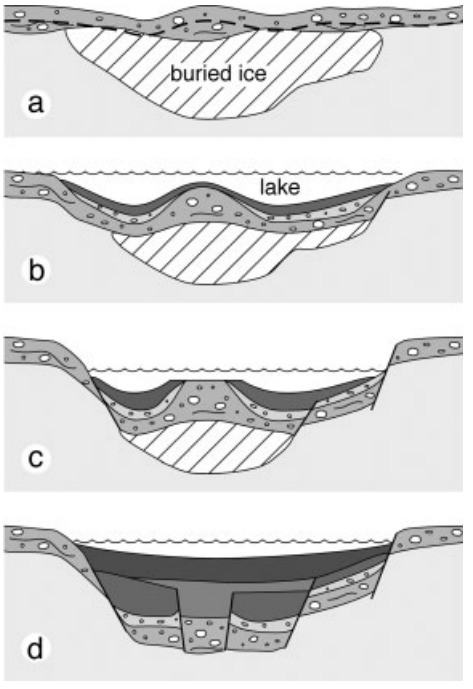

Figure 11 Cartoon of the development of a dead-ice lake in the Pechora Lowland. (a) Initial stage where dead ice is covered by ablation till and soliflucted sediments, and is included in permafrost. Dashed line indicates depth of the active layer. (b) Onset of melting of permafrost and thus of the dead ice, creating a depression into which unstable sediments flow in the first stage of sedimentation. Later the deposition is dominated by fall-out of suspended material in the lake. (c) Further melting of the buried ice has led to a collapse of the overlying sediments. Lowering of lake-level results from downcutting of the threshold or lowering of the ground-water table. Positive features on the lake floor are eroded. (d) Final stage where all the buried ice has melted. As the dead ice melted the lake floor sunk at different locations causing the stratigraphical units to differ in thickness

The complex stratigraphy of the silt unit (B) in Lake Kormovoye is interpreted as a result of the development of mini-scale ridges and basins at the lake bottom. Probably variation in sediment thickness led to differential melting of the dead ice beneath (Paul, 1983; Benn and Evans, 1998). Erosion occurred in upstanding areas and redeposition in small depressions. Then melting increased where the sediment cover became thinner, and the former positive relief developed into depressions (Fig. 11). Several inversions of the lake bottom topography took place in Lake Kormovoye, yielding the complex stratigraphy of unit B (Fig. 3). We also assume that some of the lowering of the ice surface propagated upwards as faults in the sediment sequences (Fig. 11) because there are such large differences between nearby cores.

Indications of differential thawing of buried glacier ice has not been observed in Lake Oshkoty and it is possible to correlate the cores over distances of at least 1.3 km, suggesting more or less continuous sedimentation. The bottom of Lake Oshkoty is interpreted to have subsided gradually as the buried glacier ice melted, increasing the depth as indicated by deeper water facies overlying shallower water facies (Fig. 7).

Timing of lake formation

The lower part of the lacustrine sediments in lakes Oshkoty and Kormovoye are dated to 12.3 and 11.6 kyr BP respectively (Table 1), and in Lake Lyadhei-To to ca. 9.5 kyr BP (Wischer *et al.*, 2001). As pointed out in the discussion of the lakes Kormovoye and Oshkoty, there may be further diamictic beds and lake deposits below the coring depth, thus the basal dates of cored lakes can give only minimum ages of lake formation. Similar basal dates around 13–8 ka are obtained from other lakes in the Pechora Lowland. The oldest date is 12.9 kyr BP from laminated lacustrine mud along the More-Yu River (Astakhov, 2001), whereas a small lake near Vastiansky Kon is dated to 9.6 ka (Tveranger *et al.*, 1995) and Lake Mitrophan is dated to around 9 ka (Davydova *et al.*, 1992; Davydova and Servant-Vildary, 1996) (Fig. 1). At Markhida dates below and above deformed lacustrine sediments deposited during melting of buried ice have given ages of 9.4–8.7 ka (Tveranger *et al.*, 1995). At the Bolvan Bog on the Timan Ridge (Fig. 1) dead ice started to melt around 13–10 ka forming a large palaeolake. After downcutting of the outlet sand the last dead ice remains melted about 8.3 ka, creating the present lake basins (Paus *et al.*, in press).

In the Pechora Lowland, all the above-mentioned lakes have yielded similar basal dates between 13 and 9–8 kyr BP, which indicate that the melting of buried ice started during the warming at the onset of the Bølling and accelerated at the beginning of the Holocene. Similar dates also have been obtained on the Yugorski Peninsula (Manley *et al.*, 2001) and western areas in Russia affected by the Scandinavian ice-sheet (e.g. Arslanov *et al.*, 1992a,b; Davydova and Servant-Vildary, 1996; Davydova *et al.*, 1996; Elina and Filimonova, 1996; Lysså *et al.*, 2001; Subetto *et al.*, 2002).

Landscape development

The formation of a dead-ice hummocky terrain can be considered to consist of three stages (Clayton, 1964): (i) the actively moving glacier; (ii) cessation of the movement and melting of the surficial ice; (iii) final melting of the deepest buried ice.

The last ice advance in the eastern and central part of the Pechora Lowland is dated to 90–80 ka by many OSL dates on beach sediments from the ice-dammed Lake Komi (Fig. 12a) (Mangerud *et al.*, 2001, in press). This should be the relevant age for stage 1 for all sites described above. A younger advance to the Markhida Moraine is dated to 60–50 ka, but was apparently restricted to the northwest part of the lowland (Fig. 1).

The youngest date from kame sediments near Lyadhei-To suggests that the downwasting of surficial ice started immediately after the ice advance and created a hummocky landscape. At ca. 80 ka most of the surficial ice must have melted away, Lake Komi drained and normal fluvial drainage was established, as indicated by the dates from Syateittyvis (Fig. 10). Similar dates on fluvial sand also have been obtained at Hongurei (Henriksen *et al.*, 2001) and Vastiansky Kon (Tveranger *et al.*, 1998) (Fig. 1). Probably only ice buried deeper than the active layer of the permafrost survived longer (Fig. 12b). Deglaciation shortly after the ice advance is in agreement with the ice-sheet reconstruction by Tveranger *et al.* (1999), who postulated a thin, short-lived ice sheet and rapid stagnation.

The length of time from glacial stagnation to the final melting of buried glacier ice varies considerably. In Iceland a period of 50–60 yr is reported for presently retreating glaciers (Krüger and Kjær, 2000), whereas buried ice disintegrated over a period of 7000–9000 yr during the Late Wisconsin in Minnesota, USA (Florin and Wright, 1969; Wright, 1980). In the Pechora Lowland the final melting of the deepest buried ice occurred at 13–8 ka, i.e. 80 kyr after deglaciation, resulting in the fresh hummocky topography with numerous lakes as seen today (Fig. 12c). The simplest interpretation of our observation is that there was stable permafrost throughout the Middle and Late Weichselian until about 13 ka. Thus the buried glacier ice survived for a period of ca. 80 000 yr in the eastern and central part of the Pechora Lowland. In the western part the buried ice survived for ca. 50 000 yr as it has been affected by a 60 ka glacial advance (Mangerud *et al.*, 2001). Obviously, glacier ice buried below the active layer in permafrost regions will not melt until the permafrost melts. Pleistocene glacier ice still exist in the permafrost in the Canadian Arctic (e.g. French and Harry, 1988; Worsley, 1999), Greenland (Houmark-Nielsen *et al.*, 1994), in many areas in Siberia (e.g. Kaplanskaya and Tarnogradskiy, 1986; Astakhov and Isayeva, 1988; Vaikmäe *et al.*, 1993; Forman *et al.*, 1999; Alexanderson *et al.*, 2001; Manley *et al.*, 2001) and even in the northern part of the Pechora Lowland (Astakhov *et al.*, 1999, p. 35). In Antarctica there is even glacier ice from the Miocene (Sugden *et al.*, 1995).

The thickness of sediment cover has simply exceeded the depth of the active layer so the buried ice masses have become a part of the permafrost (Paul, 1983; Benn and Evans, 1998). Melting started at the climatic amelioration at the transition to the Holocene. That permafrost started to melt at that time is also seen from dates of organic matter in ice-wedge casts. Along the Shapkina River such ^{14}C dates yielded 11.3, 10.2 and 9.5 kyr BP, a date of 10.3 kyr BP was obtained from Nyiezniy Dvoinic (Fig. 1 and Table 1), and a date of 12.3 kyr BP from Kuya Bridge (Mangerud *et al.*, 1999). Also, the flow-till beds at Markhida dated to 10.1–8.7 kyr BP indicate permafrost melting (Tveranger *et al.*, 1995). Most of the dead ice seems to have disappeared by 9–8 ka. The duration of the final melting of the buried glacier ice varied from a few hundred years at Markhida (Tveranger *et al.*, 1995) to at least 2000–3000 yr beneath Lake Kormovoye.

An important lesson from this study is that a fresh glacial landscape may not necessarily imply recent deglaciation, but permafrost melting. This is especially relevant here, because the fresh landscape of the Pechora Lowland is continuous with

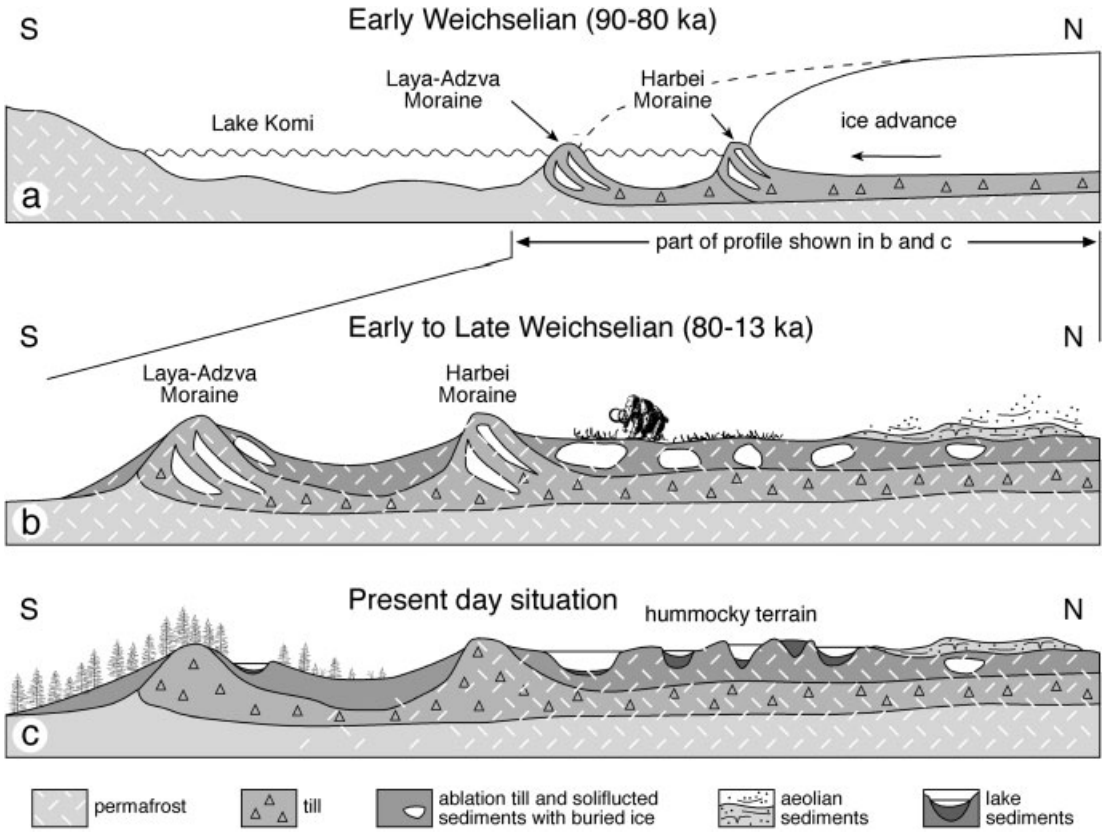

Figure 12 Idealised evolution of the landscape in the Pechora Lowland. (a) During the Early Weichselian (90–80 ka), the Barents–Kara ice-sheet dammed the proglacial Lake Komi and formed push-moraines including slabs of ice. (b) Dead ice in the glaciated, northern part of the profile in (a) became buried beneath sediments, mainly ablation till and solifluction deposits, in the Early to Late Weichselian (80–13 ka). During this time span, periods with tundra steppe and presence of mammoths and other megafaunas were interspersed with dry periods of widespread aeolian sedimentation (Mangerud *et al.*, 1999). (c) During the early Holocene most of the buried glacier ice had melted creating numerous lakes. In the northernmost part where permafrost was more persistent buried ice survived for a longer time, even during the Holocene climatic optimum

the similar landscape of the Baltic–German area, deglaciated from the Scandinavian ice-sheet 60–70 kyr later.

Climatic implications

The climate from the last glaciation at about 90 ka until the melting of buried ice at 13–9 ka varied between cold, dry conditions with deposition of aeolian sand to warmer intervals with treeless steppe and presence of megafauna such as mammoths, and even humans (Fig. 12b) (Mangerud *et al.*, 1999; Pavlov *et al.*, 2001). The survival of dead ice during this 80 000 yr period indicates that at no time was the climate warm enough to melt the buried ice. Thus permafrost has prevailed in the vast area of the Pechora Lowland throughout the Middle and Late Weichselian until the warming of the late-glacial interstadials and early Holocene.

Conclusion

1 Melting of surficial ice started soon after the regional deglaciation around 90 ka, and was completed a few thousand years later.
2 Melting of buried glacier ice, which resulted in many of the lakes in the Pechora Lowland, started as a result of climatic warming around 13–9 ka, indicating that the dead ice survived in the permafrost for a period of 50 000–80 000 yr.
3 The fresh looking glacial landscape of Pechora Lowland, with numerous lakes, results from degradation of permafrost.
4 Differential melting of buried glacier ice can cause extremely complex sedimentation with concurrent deposition and erosion.

Acknowledgements Andrei Monayev and the Usinsk Division of the Polar Ural Geological Expedition organised transport and the coring operations, Conoco/Arkhangelsk Oil at the Ardalin oil field (Polar Light) helped with transport and accommodation during the Oshkoty field expedition. Olga Maslenikova, Frank Wischer and Wolf-Dieter Hermichen were good company in the field around Lyadhei-To, Valery Astakhov helped with organising the field expeditions and provided valuable discussions, Hilary H. Birks helped with analysis of macrofossils for AMS dating, Reidar Løvlie analysed magnetic susceptibility, Jane Ellingsen and Eva Bjørseth helped with the figures, Jan Berge prepared the pollen samples, Beate Ingvartsen drew the pollen diagram. Brian Robins corrected the English language. Øystein Lohne and Ståle Raunholm provided comments on the manuscript. Dmitri Subetto and an anonymous referee provided constructive remarks on the manuscript. To all these persons and institutions we give our sincere thanks.

This paper is a contribution to the Russian–Norwegian interdisciplinary project Paleo Environment and Climate History of the Russian Arctic (PECHORA) funded by the Research Council of Norway, and to the project Ice Sheets and Climate in the Eurasian Arctic at the Last Glacial maximum (Eurasian Ice Sheets, Contract no. ENV4-CT97-0563) of the EC Environment and Climate Research Programme. Both projects are co-ordinated by the European Science Foundation research programme Quaternary Environments of the Eurasian North (QUEEN).

References

Alexanderson H, Hjort C, Möller P, Antonov O, Pavlov M. 2001. The North Taymyr ice-marginal zone, Arctic Siberia—a preliminary overview and dating. *Global and Planetary Change* **31**: 427–445.

Arslanov KhA, Davydova NN, Nedogarko IV, Subetto DA, Khomutova VI. 1992a. Valday Lake. In *The History of Lakes of the East European Plain*, Davydova NN (ed.). Nauka: St Petersburg; 79–93. (In Russian.)

Arslanov KhA, Davydova NN, Subetto DA, Khomutova VI. 1992b. Karelian Isthmus. In *The History of Lakes of the East European Plain*, Davydova NN (ed.). Nauka: St Petersburg; 50–77. (In Russian.)

Astakhov V. 2001. The stratigraphic framework for the Upper Pleistocene of the Russian Arctic: changing paradigms. *Global and Planetary Change* **31**: 283–295.

Astakhov VI, Isayeva LL. 1988. The 'Ice Hill': an example of 'retarded deglaciation' in Siberia. *Quaternary Science Reviews* **7**: 29–40.

Astakhov VI, Svendsen JI, Matiouchkov A, Mangerud J, Maslenikova O, Tveranger J. 1999. Marginal formations of the last Kara and Barents ice sheets in northern European Russia. *Boreas* **28**: 23–45.

Baulin VV, Belopukhova YeB, Danilova NS. 1984. Holocene permafrost in the USSR. In *Late Quaternary Environments of the Soviet Union*, Velichko AA, Wright HE, Jr, Barnosky CW (eds). University of Minnesota Press: Minneapolis; 87–91.

Benn DI, Evans DJA. 1998. *Glaciers and Glaciation*. Arnold: London.

Brown J, Ferrians OJ, Jr, Heginbottom JA, Melnikov ES. 1997. *Circum-Arctic map of Permafrost and Ground-ice Conditions*. 1:10,000,000 Map CP-45, U.S. Geological Survey: Reston, VA.

Clayton L. 1964. Karst topography on stagnant glaciers. *Journal of Glaciology* **5**: 107–112.

Davydova N, Servant-Vildary S. 1996. Late Pleistocene and Holocene history of the lakes in the Kola Peninsula, Karelia and the northwestern part of the East European plain. *Quaternary Science Reviews* **15**: 997–1012.

Davydova NN, Delusina IV, Subetto DA. 1992. Bolshezemelskaya tundra. In *The History of Lakes of the East European Plain*, Davydova NN (ed.). Nauka: St Petersburg; 35–45. (In Russian.)

Davydova NN, Arslanov KhA, Khomutova VI, Krasnov II, Malakhovsky DM, Saarnisto M, Saksa AI, Subetto DA. 1996. Late- and postglacial history of lakes of the Karelian Isthmus. *Hydrobiologia* **322**: 199–204.

Elina GA, Filimonova LV. 1996. Russian Karelia. In *Palaeoecological Events during the Last 15 000 Years: Regional Syntheses of Palaeoecological Studies of Lakes and Mires in Europe*, Berglund BE, Birks HJB, Ralska-Jasiewiczowa M, Wright HE (eds). Wiley: Chichester.

Fægri K, Iversen J. 1989. *Textbook of Pollen Analysis*, 4th edn, Fægri K, Kaland PE, Krzywinski K (eds). Wiley: Chichester.

Florin M, Wright HE, Jr. 1969. Diatom evidence for the persistence of stagnant glacial ice in Minnesota. *Geological Society of America Bulletin* **80**: 695–704.

Forman SL, Ingolfsson O, Gataullin V, Manley WF, Lokrantz H. 1999. Late Quaternary stratigraphy of western Yamal Peninsula, Russia: new constraints on the configuration of the Eurasian ice sheet. *Geology* **27**: 807–810.

French HM, Harry DG. 1988. Nature and origin of ground ice, Sandhills Moraine, southwest Banks Island, western Canadian Arctic. *Journal of Quaternary Science* **3**: 19–30.

Gataullin V, Mangerud J, Svendsen JI. 2001. The extent of the Late Weichselian ice sheet in the southeastern Barents Sea. *Global and Planetary Change* **31**: 453–474.

Henriksen M, Mangerud J, Maslenikova O, Matiouchkov A, Tveranger J. 2001. Weichselian stratigraphy and glaciotectonic deformation along the lower Pechora River, Arctic Russia. *Global and Planetary Change* **31**: 297–319.

Houmark-Nielsen M, Hansen L, Jørgensen ME, Kronborg C. 1994. Stratigraphy of a Late Pleistocene ice-cored moraine at Kap Herschell, Northeast Greenland. *Boreas* **23**: 505–512.

Kaplanskaya FA, Tarnogradskiy VD. 1986. Remnants of the Pleistocene ice sheets in the permafrost zone as an object for paleoglaciological research. *Polar Geography and Geology* **10**: 257–266.

Khotinskiy NA. 1984. Holocene vegetation history. In *Late Quaternary Environments of the Soviet Union*, Velichko AA, Wright HE, Jr, Barnosky CW (eds). University of Minnesota Press: Minneapolis; 179–200.

Kremenetski CV, Sulerzhitsky LD, Hantemirov R. 1998. Holocene history of the northern range limits of some trees and shrubs in Russia. *Arctic and Alpine Research* **30**: 317–333.

Krüger J, Kjær KH. 2000. De-icing progression of ice-cored moraines in a humid, subpolar climate, Kötlujökull, Iceland. *The Holocene* **10**: 737–747.

Lysså A, Demidov I, Houmark-Nielsen M, Larsen E. 2001. Late Pleistocene stratigraphy and sedimentary environment of the Arkhangelsk area, northwest Russia. *Global and Planetary Change* **31**: 179–199.

MacDonald GM, Velichko AA, Kremenetski CV, Borisova OK, Goleva AA, Andreev AA, Cwynar LC, Riding RT, Forman SL, Edwards TWD, Aravena R, Hammarlund D, Szeicz JM, Gattaulin VN. 2000. Holocene treeline history and climate change across northern Eurasia. *Quaternary Research* **53**: 302–311.

Mackay JR, Dallimore SR. 1992. Massive ice of the Tuktoyaktuk area, western Arctic coast, Canada. *Canadian Journal of Earth Science* **29**: 1235–1249.

Mangerud J, Svendsen JI, Astakhov VI. 1999. Age and extent of the Barents and Kara ice sheets in Northern Russia. *Boreas* **28**: 46–80.

Mangerud J, Astakhov VI, Murray A, Svendsen JI. 2001. The chronology of a large ice-dammed lake and the Barents-Kara ice sheet advances, northern Russia. *Global and Planetary Change* **31**: 321–336.

Mangerud J, Jakobsson M, Alexanderson H, Astakhov V, Clarke GKC, Henriksen M, Hjort C, Krinner G, Lunkka JP, Möller P, Murray A, Nikolskaya O, Saarnisto M, Svendsen JI. In press. Ice-dammed lakes and rerouting of the drainage of Northern Eurasia during the last glaciation. *Quaternary Science Reviews*.

Manley WF, Lokrantz H, Gataullin V, Ingólfsson Ó, Forman SL, Andersson T. 2001. Late Quaternary stratigraphy, radiocarbon chronology, and glacial history at Cape Shpindler, southern Kara Sea, Arctic Russia. *Global and Planetary Change* **31**: 239–254.

Murray AS, Wintle AG. 2000. Luminescence dating of quartz using an improved single-aliquot regenerative-dose protocol. *Radiation Measurements* **32**: 57–73.

Murray AS, Marten R, Johnston A, Martin P. 1987. Analysis for naturally occurring radionuclides at environmental concentrations by gamma spectrometry. *Journal of Radioanalytical and Nuclear Chemistry, Articles* **115**: 263–288.

Murton JB. 1996. Thermokarst-lake-basin sediments, Tuktoyaktuk Coastlands, western Arctic Canada. *Sedimentology* **43**: 737–760.

Nelson RE, Carter LD, Robinson SW. 1988. Anomalous radiocarbon ages from a Holocene detrital organic lens in Alaska and their implications for radiocarbon dating and paleoenvironmental reconstructions in the Arctic. *Quaternary Research* **29**: 66–71.

Olley JM, Murray AS, Roberts RG. 1996. The effects of disequilibria in the uranium and thorium decay chains on burial dose rates in fluvial sediments. *Quaternary Science Reviews* **15**: 751–760.

Paul MA. 1983. The supraglacial landsystem. In *Glacial Geology*, Eyles N (ed.). Pergamon Press: Oxford; 71–90.

Paus Aa, Svendsen JI, Matioushkov A. In press. Late Weichselian (Valdaian) and Holocene vegetation and environmental history of the Timan Ridge, European Arctic Russia. *Quaternary Science Reviews*.

Pavlov P, Svendsen JI, Indrelid S. 2001. Human presence in the European Arctic nearly 40,000 years ago. *Nature* **413**: 64–67.

Polyak L, Gataullin V, Okuneva O, Stelle V. 2000. New constrains on the limits of the Barents-Kara ice sheet during the Last Glacial Maximum based on borehole stratigraphy from the Pechora Sea. *Geology* **28**: 611–614.

Rampton VN. 1973. The history of thermokarst in the Mackenzie-Beaufort regions, Northwest Territories Canada. *International Union of Quaternary Research, 9th Congress, Christchurch, New Zealand, 2–10 December 1973, Abstract*: 299.

Rampton VN. 1988. Quaternary geology of the Tuktoyaktuk Coastlands, Northwest Territories. *Geological Survey of Canada, Memoir* **423**; 98pp.

Stuiver M, Reimer PJ. 1993. Extended ^{14}C database and revised CALIB radiocarbon calibration program. *Radiocarbon* **35**: 215–230.

Stuiver M, Reimer PJ, Bard E, Beck JW, Burr GS, Hughen KA, Kromer B, McCormac FG, van der Plicht J, Spurk M. 1998. INTCAL98

Radiocarbon age calibration 24,000–0 cal BP. *Radiocarbon* **40**: 1041–1083.

Subetto DA, Wohlfarth B, Davydova NN, Sapelko TV, Björkman L, Solovieva N, Wastegård S, Possnert G, Khomutova VI. 2002. Climate and environment on the Karelian Isthmus, northwestern Russia, 13 000–9000 cal. yrs BP. *Boreas* **31**: 1–19.

Sugden DE, Marchant DR, Potter N, Jr, Souchez RA, Denton GH, Swisher CC, Tison JL. 1995. Preservation of Miocene glacier ice in East Antarctica. *Nature* **376**: 412–414.

Svendsen JI, Astakhov VI, Bolshiyanov DYu, Demidov I, Dowdeswell JA, Gataullin V, Hjort C, Hubberten HW, Larsen E, Mangerud J, Melles M, Möller P, Saarnisto M, Siegert MJ. 1999. Maximum extent of the Eurasian ice sheets in the Barents and Kara Sea region during the Weichselian. *Boreas* **28**: 234–242.

Tveranger J, Astakhov V, Mangerud J. 1995. The margin of the last Barents–Kara Ice Sheet at Markhida, northern Russia. *Quaternary Research* **44**: 328–340.

Tveranger J, Astakhov V, Mangerud J, Svendsen JI. 1998. Signature of the last shelf-centred glaciation at a key section in the Pechora Basin, Arctic Russia. *Journal of Quaternary Science* **13**: 189–203.

Tveranger J, Astakhov V, Mangerud J, Svendsen JI. 1999. Surface form of the south-western sector of the last Kara Sea Ice Sheet. *Boreas* **28**: 81–91.

Vaikmäe R, Michel FA, Solomatin VI. 1993. Morphology, stratigraphy and oxygen isotope composition of fossil glacier ice at Ledyanaya Gora, Northwest Siberia, Russia. *Boreas* **22**: 205–213.

Väliranta M, Kaakinen A, Kuhry P. 2003. Holocene climate and landscape evolution east of the Pechora Delta, East-European Russian Arctic. *Quaternary Research* **59**: 335–344.

Wischer F, Andreev A, Hermichen WD, Hubberten HW. 2001. The Late-Quaternary environmental history of the western foreland of the Polar Urals inferred from lake sediment studies. *EUG XI, Journal of Conference Abstracts* **6**: 217.

Worsley P. 1999. Context of relict Wisconsinan glacial ice at Angus Lake, SW Banks Island, western Canadian Arctic and stratigraphic implications. *Boreas* **28**: 543–550.

Wright HE, Jr. 1980. Surge moraines of the Klutlan Glacier, Yukon Territory, Canada: origin, wastage, vegetation succession, lake development, and application to the late-glacial of Minnesota. *Quaternary Research* **14**: 2–18.